Optimizing Material Properties and Geometry of a Physical Multi-Layered Vocal Fold Model

B. Schmidt[1], G. Leugering[2], M. Döllinger[3], R. Lerch[4], M. Kaltenbacher[5], M. Stingl[6]

[1] *University of Erlangen-Nuremberg, Germany, Bastian.Schmidt@am.uni-erlangen.de*

[2] *University of Erlangen-Nuremberg, Germany, leugering@am.uni-erlangen.de*

[3] *University of Erlangen-Nuremberg, Germany, Michael.Doellinger@uk-erlangen.de*

[4] *University of Erlangen-Nuremberg, Germany, reinhard.lerch@lse.e-technik.uni-erlangen.de*

[5] *Alpds-Adriatic University of Klagenfurt, Austria, Manfred.Kaltenbacher@uni-klu.ac.at*

[6] *University of Erlangen-Nuremberg, Germany, stingl@am.uni-erlangen.de*

Introduction

Understanding the physical fundamentals of human voice generation is a challenging and interdisciplinary task. The present work takes a closer look at a self-sustained physical model of the human larynx, in which the vocal folds are modeled by multi-layered elastic bodies, i.e. silicone layers. We search for optimal material and geometry parameters in the sense that the deformation of the multi-layer model at its surface is as similar to given deformation patterns arising from hemilarynx experiments as possible. For this purpose, we employ an optimization concept based on a finite element simulation in which the vocal fold is modeled as linear elastic body. We use the material optimization approach [3] in order to identify optimal material parameters and employ techniques from shape optimization [10], in order to optimize geometry of the boundaries between the different layers. We conclude this presentation by giving some numerical results using a 2D vocal fold model.

Hemilarynx Experiments

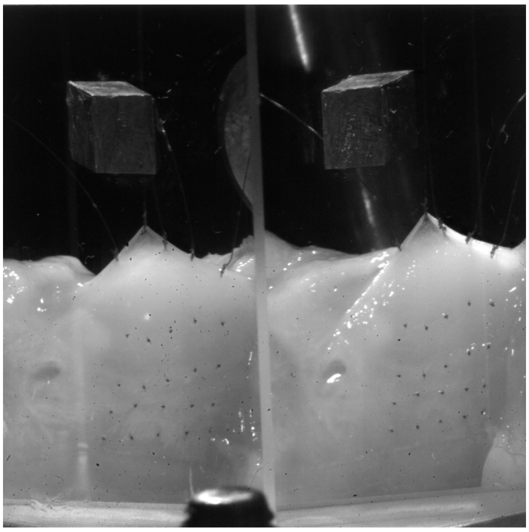

Figure 1: Two view photograph of the vocal fold with sutures and applied force

An excised human larynx was obtained from the autopsy unit of the UCLA Medical Center. It was quick-frozen with liquid nitrogen to maintain tissue properties [5], stored in $-20°C$ freezer for 6 months, and defrosted the day before the experiment. A detailed description of the set-up was given previously [6]. The creation of a hemilarynx required the removal of one (i.e. right) vocal fold. The trachea was mounted over a stainless steel cylindrical tube with an inner diameter of $8mm$. A glass plate was attached at the top of the tube. To track the movements of the medial surface of the vocal fold, 25 surgical microsutures were mounted, see figure 1. To avoid any disturbance of the natural material characteristics of the vocal fold, the sutures were positioned to penetrate only the mucosal epithelium and not the superficial layer [4]. Deformations of the vocal fold were induced by rotational pulling of the most upper sutures with different weights. The deformations were imaged with a digital camera. A right-angle prism was placed at the glass plate, opposite the vocal fold, simulating two camera views, a necessary condition to compute three-dimensional coordinates from a two-dimensional recording [1]. For later calibration, a brass cube ($5mm^3$) was glued to the glass plate superior to the vocal fold [7, 8]. The tracking of suture positions and the computation of the physical coordinates was performed using a linear transformation method [7].

General Problem Setup

Let $\Omega \subset \mathbb{R}^d$ with $d \in \{2, 3\}$ denote an elastic body with Lipschitz boundary $\Gamma = \partial\Omega$. On Ω, we consider the following boundary value problem of linear elasticity: Find a displacement field $u \in H^1(\Omega; \mathbb{R}^d)$ such that

$$\begin{aligned} -\mathrm{div}(\sigma) &= 0 && \text{in } \Omega \\ \sigma \cdot n &= f && \text{on } \Gamma_F \\ u &= 0 && \text{on } \Gamma_0 \\ \sigma &= E \cdot e(u) && \text{in } \Omega\,. \end{aligned} \tag{1}$$

Here $f \in L^2(\Gamma_F; \mathbb{R}^d)$, $\Gamma_F \subset \Gamma$ is a given surface force and $L^2(\Omega; \mathbb{R}^d)$ denotes the space of quadratically integrable functions on Ω, which takes values in $\mathbb{R}^d$. When loaded by f the elastic body is deformed; the corresponding displacement field is denoted by $u \in \mathcal{H} := H^1(\Omega; \mathbb{R}^d)$, where $H^1 \subset L^2(\Omega)$ is the Sobolev space of quadratically integrable functions with weak derivatives. Associated with the displacement field is the (small) strain tensor given as $e(u) = \frac{1}{2}(\nabla u + \nabla u^\top) \in L^2(\Omega; \mathbb{R}^{d \times d})$. We assume that the body is made of elastic material, characterized by a material tensor $C \in L^\infty(\Omega;\mathbb{R}^{d\times d\times d\times d})$. Finally the strain tensor is related to the stress tensor by Hooke's Law $\sigma = C \cdot e(u) \in L^\infty(\Omega;\mathbb{R}^{d\times d})$.

As the material tensor as well as the strain and stress tensors fulfill some symmetry properties, we can define $d' := \frac{1}{2}d(d+1)$ and rewrite $e \in L^2(\Omega;\mathbb{R}^{d'})$, $\sigma \in L^\infty(\Omega;\mathbb{R}^{d'})$, as well as $C \in L^\infty(\Omega;\mathcal{S}^{d'})$, where $\mathcal{S}^{d'}$ is the space of all symmetric $d' \times d'$−matrices.

In the context of optimization it has certain advantages to work with the weak formulation of partial differential equations. For this purpose, we state the weak form of system (1): *find* $u \in \mathcal{H}_0 := \{u \in \mathcal{H} | u_{\Gamma_0} = 0\}$, *s.t.*

$$\underbrace{\int_\Omega \langle C(x)e(u)(x), e(v)(x)\rangle \mathrm{d}x}_{a_C(u,v)} = \underbrace{\int_\Gamma f(x)^\top v(x)\mathrm{d}x}_{l(v)} \quad \forall v \in \mathcal{H}_0. \tag{2}$$

Material Optimization

Based on this PDE (2) we consider the following problem:

Given a deformation $u_0 \in L^2(\Gamma_T)$ on a part of the boundary and given a force f applied to the body $\Omega = \bigcup_i \Omega_i$ consisting of a defined number of layers Ω_i, find a material C_{α_i} uniquely defined by a parameter set α_i for each layer, which generates a deformation u^* as close as possible to the given deformation u_0.

In our particular application, the given boundary deformation arises from the hemilarynx experiments. In detail, we formulate this optimization problem as follows:

$$\begin{aligned} \min_{\alpha\in\mathcal{A}} \quad & J(\alpha) := \tfrac{1}{2}\|u-u_0\|^2_{\Gamma_T} \qquad (3)\\ \text{s.t.} \quad & \mathrm{vol}(\alpha) = V \\ & a_{C_\alpha}(u,v) = l(v) \quad \forall v \in \mathcal{H}_0 \end{aligned}$$

Here the 'volume' of the material is defined as

$$\mathrm{vol}(\alpha) = \int_\Omega \mathrm{Tr}(C_\alpha(x))\mathrm{d}x \tag{4}$$

a measure for the over-all stiffness of the material. The set of *admissible material parameters* $\mathcal{A}$ consists of all parameter sets, which are constant on each of the layers, i.e.

$$\mathcal{A} = \{\alpha \in L^\infty(\Omega)^p, \alpha(x) = \alpha_i \forall x \in \Omega_i, \alpha_i \in X_i \subseteq \mathbb{R}^p\} \tag{5}$$

where $X_i \subseteq \mathbb{R}^p$ contains all allowed material parameters and has to guarantee that C_α is positive definite on Ω.

Remark. Problem (3) falls into the general class of design problems; for a survey see [3, 10] and the references therein. Moreover due to the tracking functional $J(u) = \frac{1}{2}\|u-u_0\|^2_{\Gamma_T}$ problem (3) is a so called inverse problems ([9]). Inverse problems are known to be *ill-posed*. This is the reason, why typically a regularization term is added to the objective functional. In our case the volume functional (4) acts as a regularization.

This formulation allows for different material laws (e.g. isotropic, orthotropic, anisotropic) to be used in the optimization process. We use transversal-isotropic material aligned to the coordinate-axes (see, e.g. [11]) for our vocal fold model simulation. The isotropic plane lies in vertical and lateral direction. The transversal-isotropic material depends on 5 parameters $E_{\mathrm{iso}}, \nu_{\mathrm{iso}}, G_{\mathrm{io}}, E_{\mathrm{o}}, \nu_{\mathrm{oi}}$ or ν_{io} ($\nu_{\mathrm{oi}}E_{\mathrm{o}} = \nu_{\mathrm{io}}E_{\mathrm{iso}}$), which all together form the design vector α. The equations

$$\begin{aligned} &E_{\mathrm{iso}} > 0, E_{\mathrm{o}} > 0, G_{\mathrm{io}} > 0, \\ &\qquad -1 < \nu_{\mathrm{iso}} < 1, 1 - \nu - 2\nu_{\mathrm{io}}\nu_{\mathrm{oi}} > 0 \end{aligned} \tag{6}$$

guarantee positive definiteness of the material-matrix C_α.

Shape Optimization

Working with a multi-layered model, the question arises, whether by modification of the of the layer boundaries, the cost functional in problem (3) can be further improved. For this purpose, we optimize in a next step parameters which influence just geometry rather than the material. This idea leads to the following problem:

$$\begin{aligned} \min_{\beta\in X\subset\mathbb{R}^m} \quad & J(\beta) := \tfrac{1}{2}\|u-u_0\|^2_{\Gamma_T} \qquad (7)\\ \text{s.t.} \quad & C(x) = C_i \quad \text{in } \Omega_i(\beta), \bigcup_i \Omega_i(\beta) = \Omega \\ & a_C(u,v) = l(v) \quad \forall v \in \mathcal{H}_0 \end{aligned}$$

The set X consists of all feasible combinations of shape parameters and usually is a m-dimensional polyhedron, in many cases even just a m-dimensional cube. The material matrices C_i characterize the material properties each layer.

Remark. Problem (7) falls into the class of shape design problems [3, 10]. Usually only the outer boundary of the elastic body is subject to optimization, whereas here we the outer shape remains fixed, whereas the geometry of the inner boundary layers is varied.

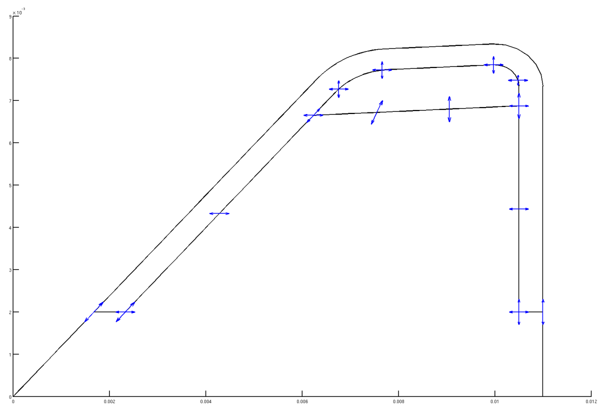

Figure 2: Control points for splines defining the layers in the vocal fold model

Problem (7) is given in very general form, not specifying any details on how the geometry depends on the parameter vector β. Figure 2 visualizes part of the idea we employ in (7). Our approach is based on [10], but slightly modified w.r.t. the optimization of the inner layer boundaries. We model each line separating two layers in the original vocal fold model by a set of control points (see figure 2) and associated piecewise quadratic splines. In order to avoid re-meshing and element degeneration during optimization, all grid points in a certain neighborhood of the layer boundary depend continuously and smooth on the layer boundary and are thus fully characterized by its control points. This approach leads to moderate deformations and may be considered restrictive. However in case of the vocal fold model, large changes of the boundaries are not expected.

Material and Shape Optimization

Being able to optimize material on the one hand and shape on the other hand it is apparent to think about a combination of these two processes. A corresponding problem formulation can be easily derived from (3) by introducing dependence of the layers Ω_i on the parameter β which itself is subject to optimization.

$$\min_{\substack{\beta\in X\subset\mathbb{R}^m\\ \alpha\in\mathcal{A}_\beta}} \quad J(\alpha) := \frac{1}{2}\left\|u-u_0\right\|^2_{\Gamma_T} \tag{8}$$

$$\text{s. t.} \quad \mathrm{vol}(C_\alpha) = V$$

$$a_{C_\alpha}(u,v) = l(v) \quad \forall v \in \mathcal{H}_0$$

where

$$\mathcal{A}_\beta = \{\alpha(x) = \alpha_i \forall x \in \Omega_i(\beta), \alpha_i \in X_i \subseteq \mathbb{R}^p\} \tag{9}$$

$$\bigcup_i \Omega_i(\beta) = \Omega, \forall \beta \in X. \tag{10}$$

The dependence on β is only seen in the set of admissible material parameters (9), which consists now of all material parameters that are constant on each layer $\Omega_i(\beta)$ with each layer being defined by the shape variable β.

Results

All optimization problems (3), (7) and (8) contain the PDE (1). This PDE is solved using the finite element framework CFS++ (Coupled Field Simulation++), a software package developed at the Chair of Sensor Technology at the University of Erlangen-Nuremberg. This package has been extended to communicate with the optimizer SCPIP [13], which has recently been applied in many areas of design and structural optimization. It is based on the so-called sequential convex programming concept. Furthermore functionality for calculating sensitivities of the objective function and volume constraint w.r.t. both the material and the shape parameters has been added to CFS++.

Material Optimization

Our 3D finite element model of the vocal fold is based on the model described in [2] and consists of 10512 brick elements. Boundary forces and displacements are extracted from the hemilarynx experiments. We employ a multiple load approach concentrating information from several experiments in one optimization problem. Figure 3 shows the vocal fold model deformed by the reference displacement u_0 (left) and the optimization result (right).

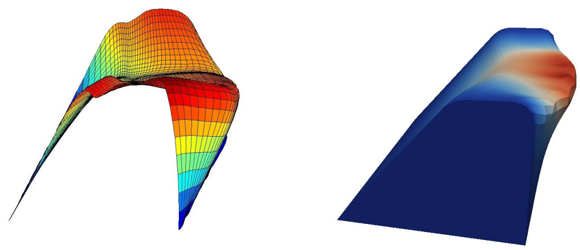

Figure 3: Result of material optimization (right) compared to the vocal fold model with reference displacement generated from data from the hemilarynx experiments (left)

Shape Optimization

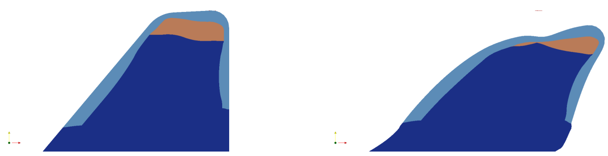

Figure 4: Result of shape optimization in original (left) and deformed (right) state with preceeding isotropic material optimization

For the purpose of simplicity, we restrict ourselves to a 2D vocal fold model subsequently. The 2D model is generated by extracting the middle-plane of the 3D vocal fold model described in the previous section. The associated mesh consists of 438 quadrilateral elements. As the vertical and lateral plane of the vocal fold model coincide with the symmetry plane of the transversal-isotropic material used in 3D, we use an isotropic material model. Here we employ the shape optimization process as a some post processing step after having optimized the material parameters. Figure 4 visualizes the results.

Material and Shape Optimization

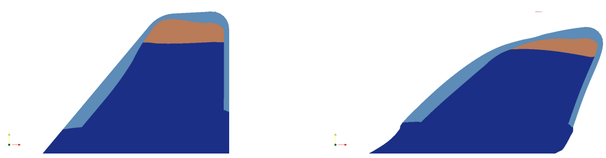

Figure 5: Result of simultaneous material and shape optimization in original (left) and deformed (right) state

Now we apply shape and material optimization techniques concurrently. The results are shown in figure 5. One can see small changes in the resulting geometry compared to successive material and shape optimization (cf. figure 4). A comparison of the optimal displacements achieved by the methods 'pure material optimization', 'successive material and shape optimization' and 'concurrent material and shape optimization' is depicted in figure 6 and corresponding objective values given table 1. In addition figure 6 shows four reference curves: The un-deformed boundary of the 2D vocal fold model, the boundary deformed by the reference displacement u_0, a deformation result obtained using material parameters found in literature and a result obtained by so called

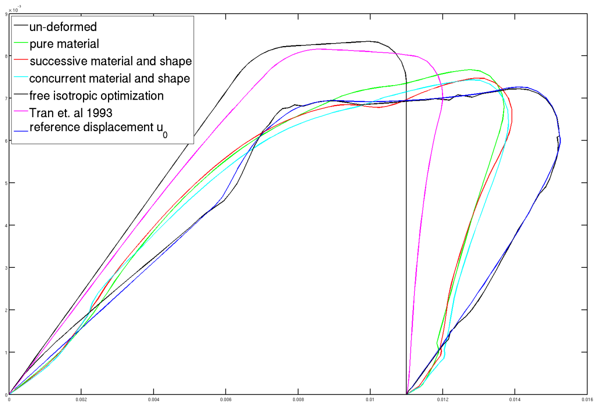

Figure 6: Comparison of achieved displacements for the different optimization methods.

optimization method	obj. function value	max. tracking distance (mm)
Tran et al.	$2.04 \cdot 10^{-4}$	3.44
just material	$9.72 \cdot 10^{-5}$	1.88
shape after material	$8.26 \cdot 10^{-5}$	1.75
shape and material	$8.06 \cdot 10^{-5}$	1.70
free material	$2.96 \cdot 10^{-6}$	0.60

Table 1: Objective function value and maximal tracking distance, i.e. the maximal distance considering the displacement of all points on the surface compared to the reference displacement.

free isotropic material optimization. For generating the displacement curve using material parameters from literature we applied the (constant) Young's modulus of $1.26kPa$ found in [12] to every layer in our numerical vocal fold model and performed a simulation step using the boundary forces extracted from the hemilarynx experiment. In free isotropic material optimization, we allow the material properties to vary from element to element throughout the entire vocal fold. The results obtained from free material optimization typically lead to materials which are hard to manufacture. On the other hand these materials are often used as benchmark materials showing how far one is from the 'ultimate' solution or in order to gain more insight in the structure of optimal materials.

Conclusion

The vocal fold deformations measured in the hemilarynx experiments do not correspond very well to the material parameters known from literature. We use a mathematical approach in order to find material parameters generating boundary displacements, which match the measured deformations as close as possible. Optimizing material parameters in our multi-layered vocal fold model already generates a much better result. It turns out that using shape optimization and thus allowing moderate changes in the geometry of the material layers, leads to further improvement while keeping the vocal fold model simple enough for the manufacturing process. The best results are achieved by simultaneous material and shape optimization. The optimized material and shape parameters obtained in this way lead to a quite satisfactory accordance with the displacements measured in the hemilarynx experiments. On the other hand, the benchmark against the free material optimization result shows that there is still room for improvements. In particular the 'free material distribution' suggests that the shape optimization process may be too restrictive and that the layer geometry has to be changed more radically. This suggestion will be followed in a forthcoming paper.

References

[1] Y. I. Abdel-Aziz and H. M. Karara. Direct linear transformation from comparator coordinates into object spacecoordinates in close-range photogrammetry. In *Proceedings of the Symposium on Close-Range Photogrammetry*, pages 1–18, Falls Church, VA, 1971. American Society of Photogrammetry.

[2] F. Alipour, D. A. Berry, and I. R. Titze. A finite-element model of vocal-fold vibration. *J Acoust Soc Am*, 108(6):3003–3012, Dec 2000.

[3] M. P. Bendsøe and O. Sigmund. *Topology Optimization. Theory, Methods and Applications.* Springer-Verlag, Heidelberg, 2002.

[4] D. A. Berry, D. W. Montequin, and N. Tayama. High-speed digital imaging of the medial surface of the vocal folds. *J Acoust Soc Am*, 110(5 Pt 1):2539–2547, Nov 2001.

[5] Roger W Chan and Ingo R Tize. Effect of postmortem changes and freezing on the viscoelastic properties of vocal fold tissues. *Ann Biomed Eng*, 31(4):482–491, Apr 2003.

[6] Michael Doellinger and David A Berry. Visualization and quantification of the medial surface dynamics of an excised human vocal fold during phonation. *J Voice*, 20(3):401–413, Sep 2006.

[7] Michael Döllinger and David A Berry. Computation of the three-dimensional medial surface dynamics of the vocal folds. *J Biomech*, 39(2):369–374, 2006.

[8] Michael Döllinger, David A Berry, and Gerald S Berke. Medial surface dynamics of an in vivo canine vocal fold during phonation. *J Acoust Soc Am*, 117(5):3174–3183, May 2005.

[9] Heinz W. Engl, Martin Hanke, and Andreas Neubauer. *Regularization of inverse problems.* Springer Netherland, Berlin, 1996.

[10] J. Haslinger and R. Mäkinen. *Introduction to shape optimization.* SIAM, Philadelphia, PA, 2002.

[11] Manfred Kaltenbacher. *Numerical Simulation of Mechatronic Sensors and Actuators.* Springer, 2004.

[12] Q. T. Tran, G. S. Berke, B. R. Gerratt, and J. Kreiman. Measurement of young's modulus in the in vivo human vocal folds. *Ann Otol Rhinol Laryngol*, 102(8 Pt 1):584–591, Aug 1993.

[13] Ch. Zillober. *Software Manual for SCPIP 3.0*, 2004.